University of Toronto Human Powered Vehicle Design Team

Technical Report – 2010 ASME HPV Competition

Vehicle Class: SPEED.

Vehicle # : 21

1 Contents

2 Abstract

This technical report documents the design, testing and construction efforts undertaken by the University of Toronto Human Powered Design Team (HPVDT) in order to participate in the 2010 ASME HPV competition, in the Speed Class.

The goal of the project is to build a fast bike that can win the Drag and Endurance competitions, as well as train riders to be comfortable and fast on such a bike. A different goal, but just as important, is to give students a chance to learn to use advanced composite construction, to understand the challenges of building a human powered vehicle and to give them a place to display their design and building expertise.

While our goal is to eventually win the competition, in our first year we wish to build a reliable bike, that can, due to a full fairing, be fast enough for a good finish in the Drag and Endurance competitions. In the future years, as we are training more riders and we understand the design process behind building a bike better, our goal will be the first place overall.

The bike is a recumbent design, and much work and time was spent in understanding the best the best rider position for such a bike. The position of the rider determines the power delivery, the maneuverability of the bike, as well as the aerodynamic characteristics, thus being one of the main areas where performance can be gained or lost.

In order to understand the driver position inside a recumbent, and because we had no previous faired bike to test on, we developed a human model in Solidworks2010 (SW2010) which reproduced the movement of the rider as close as possible. The model was tuned according to measurements done on our main riders, and proved to have an anatomically correct pedaling motion, which was used to test different driver positions, transmission configurations and fairing designs.

The fairing will be constructed of two halves, the top half being purely for aerodynamically reasons, and the bottom half being a structural member. The bottom half has a carbon roll structure attached to it, behind and above the rider. This structure is mean to protect the rider in the event of a crash, especially a rollover. While the top half of the bike will not be structural, it will protect the rider from road rash. The bike is front wheel drive, and the entire transmission system is bolted to a aluminum structure, which is attached to the bottom fairing. This will allow the transmission to be constructed and tested independently of the carbon fiber fairing, such that the two can be developed in parallel.

While we are a new team, and started development comparatively late, we hope that a fast bike can be built in time and with the required reliability to challenge the more established teams at the 2010 ASME HPV competition.

3 Design Description

3.1 Human model

As a new team with no previously faired HPVs, the problem of fitting a human inside the fairing while clearing all the transmission elements proved daunting. The aerodynamics studies {REFS} tell us that the smallest frontal and wetted area provide the fastest designs. Designs such as Varna Diablo and Elvie II attempt to surround the riders as close as possible with the fairing. To be able to design the bike in an organized and traceable way, a human model was required. The main requirements were to be dimensionally similar to an average rider, to have an anatomically correct pedaling motion, and to allow for the design of the cockpit.

We designed a human model called HU1 in Solidworks2010 to achieve all these requirements. First, the general dimensions of the most average of our team members were tabbed and a model was constructed based on them. Side pictures were taken of the rider on the prototype bike, from the hip level, and the joint trajectories were compared with the HU1 model placed on a digital version of the prototype bike. The lengths of the limbs and the alignments of the joints were adjusted until the model matched the pictures for eight pedal positions. The width of the shoulders and hips were measured for the rider on the prototype bike.

The helmet was modeled after the Bell Faction helmet, size Small (**CPSC Bicycle Safety Standard Certified**). The helmet was measured and modeled in Solidworks2010.

Special attention was paid to the models of the feet, which need to be precise to allow the fairing to be as close as possible to the feet.

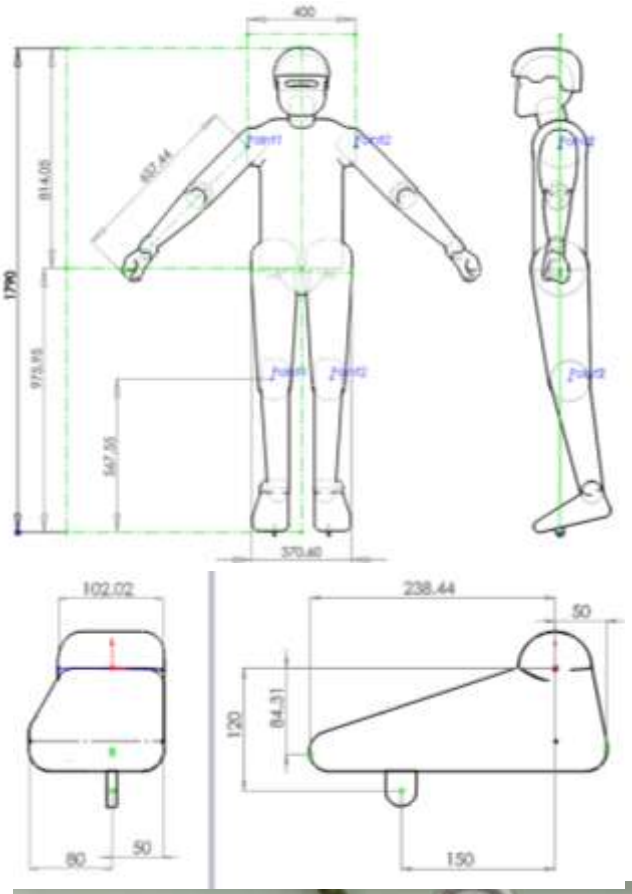

Mass		**70kg**
Degrees of freedom	**Neck/Head**	**2**
	Hip	**2**
	Knee	**1**
	Ankle	**2**
	Shoulder	**2**
	Elbow	**1**
	Hand	**2**
HU1 Height	**1780mm**	
HU1 Shoulder With	**500mm**	

HU1 MODEL

It is hoped that the HU1 model and other improved anatomic models will allow us to refine the HPV designs in the following years.

3.2 Rider positions

As we are starting the design of the HPV fresh, a variety of rider positions were considered. The main ones are:

Rider Position	Examples	Advantages	Dissadvantages
Recumbent	Varna Diablo, Rose-Hulman, Baracuda, etc	• Common, well studied • Confortable • Easier to learn to ride • Good aerodynamic configurations posible	• Posible vision problems, eyes must be above the knees. • Transmision can be dificult to package for either front or back wheel drive
Semi-upright	Road bikes, P.F.C.S.U.2.W.H.P.G.V. (2009 entry to ASME HPV)	• Most common • Most riders can already ride one • Riders can apply their maximum power • Easy to build • Simple transmision	• Aerodynamic dissadvantage • Unconfortable • Not interesting to build one.
Reverse-recumbent	ELVIE II	• Better aerodynamic advantage than recumbent • Simple transmision	• Doubtful we could find enough riders brave enough • Takes long time to learn to ride
Prone	H-Zontal	• Simple transmision • Good aerodynamics	• Takes long time to learn to ride • Not sure if any good for longer distances • Head-first not safe.

A cost analysis was performed for each configuration

Rider Position	Aerodynamics	Confort	Control	Transmision simplicity	Time to learn to ride	Rider safety	Total
Score weight	30%	10%	20%	10%	10%	20%	100%
Recumbent	**7**	**10**	**7**	**2**	**6**	**8**	**6.9**
Semi-upright	**2**	**7**	**10**	**10**	**10**	**6**	**6.5**
Reverse-recumbent	**10**	**7**	**2**	**10**	**0**	**0**	**5.1**
prone	**8**	**0**	**2**	**10**	**2**	**0**	**4**

Due to obtaining the highest score, the recumbent configuration was chosen. Next the major limitations of the recumbent configuration are investigated.

There are a number of recumbent transmission solutions to be analyzed. In order to find the fastest recumbent configuration a second table had to be devised.

Solution for Transmision	**Examples**	**Advantages**	**Dissadvantages**
FrontWheel Drive (FWD)	Varna Diablo, Rose-Hulman, Baracuda, etc	• Can mount the entire transmision on one frontal structure. • Compact • Efficient • Lightweight	• Requires a twisting chain • Can touch the driver feet during turning • Less studied
Rear Wheel Drive (RWD)	M8, Bacchetta	• Most common • Doesnt require intermediate drive • Doesnt require twisting the chain	• 3 or more pulleys • Long chain means more weight • Same steering angle as FWD, due to wheel touching the chain
Mooving Bottom Bracket (MBB)	Zockra Kouign Amann Special	• Very simple transmision • Efficient • Strong front wheel structure • Can use upper body to apply power to peddaling	• Can not make a front fairing around an EBB bike • Needs custom front wheel mount

Transimison solution	**Aerodynamics**	**Simplicity**	**Efficiency**	**Can use off-market marts**	**Total**
Score weight	30%	20%	30%	20%	100%
FWD	**10**	**6**	**7**	**8**	**7.9**
RWD	**9**	**4**	**4**	**10**	**6.7**
EBB	**3**	**10**	**10**	**2**	**6.3**

Thus, given our score analysis to find the best bicycle configuration, we decided to build a fully faired recumbent with a front wheel drive system. The fact that the fastest bike on the planet, the Varna Diablo, as well as the Rose-Hulman HPV which won last year's ASME HPV competitions, has the same configuration, reinforces our choice.

3.3 Recumbent configuration limitations

Recumbent bikes vary in configuration from radical designs such as the faired Virtual Edge, to very comfortable and simple designs, such as the Bacchetta recumbent. We started to pin down the desired configuration by analyzing the limitations presented by different locations for the seat, bottom bracket, etc.

Bottom bracket height has a minimum value dictated by the Q-factor of the cranks, lengths of the cranks, foot dimensions and the desired maximum lean angle in a turn. Given a lean angle α, a Q-factor Q , a crank length l_C , heel width w_H and distance from pedal axis to heel l_H, the minimum h height of the bottom bracket can be determined as:

$$h = \tan(\alpha)\left(\frac{Q}{2} + w_H\right) + l_H + l_C$$

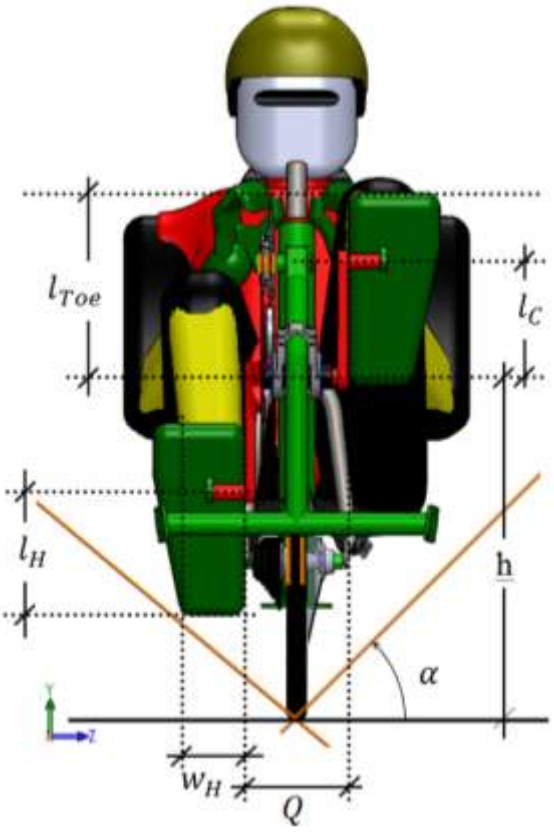

The first main limitations are the dimensions of the crank length l_C and Q-factor Q. Finding cranks shorter than 165mm is difficult and results in less efficient pedaling motion for riders used with normal (170-175mm) cranks. The Q-factor of normal cranks varies between 141mm and 151mm depending on bottom bracket and crank model, and, while it can be made smaller, it involves custom bottom bracket spindles or cranks. The measured heel to pedal spindle length is 200mm and the heel width is 80mm.

The maximum lean angle on a rowing recumbent was measured to be 23 degrees, and, from videos of past ASME HPV competitions, no angles larger than 40 degrees were observed. Given a 40 degree lean angle and the dimensions seen above, the minimum bottom bracket height was calculated to be 485mm.

The desired hip position is dictated by two variables. The first is the angle of the leg when the pedal is fully extended, which is equal to the angle of the segment defined by the bottom bracket and hip with respect to the horizontal (ϕ). The second is the length between the bottom bracket and the hip point (l_L), which is a function of the leg length and crank length.

Finding the correct angle ϕ proved to be a bit difficult, as no other conditions are found to constrain the design. A number of studies into human powered airplanes suggested an angle of -10 degrees w.r.t. horizontal, but further is necessary. The side view of the pilot needs to be analyzed.

Consider the angle ϕ of the leg with the horizontal, θ angle of the torso with the vertical, the BB to hip length l_L, torso length l_T, and shoulder to eye-level length l_E.

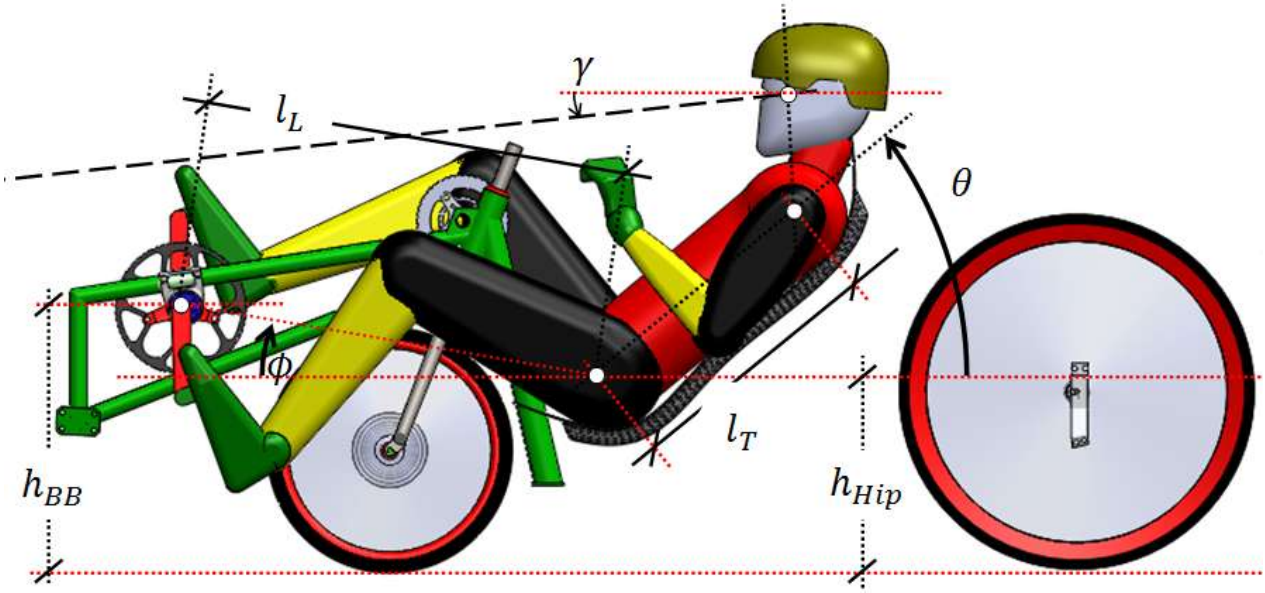

The height of the eye-level over the BB is given by the formula:

$$h_{Eye-to-BB} = -l_L \sin(\phi) + l_T \sin(\theta) + l_E$$

The horizontal distance from the BB to the level of the eyes is

$$l_{Eye-to-BB} = -l_L \cos(\phi) + l_T \cos(\theta)$$

The angle γ represents the vision angle, or how much the driver is able to see below the horizontal in front of the bike. The angle γ is a function of the angles ϕ and θ.

$$\gamma = \tan^{-1}((h_{Eye-to-BB} - l_{Toe})/ l_{Eye-to-BB})$$

l_{Toe} (see previous figure) represents the height the toe reaches above the BB.

Given a vision angle 15 degrees, which is considered minimum for a good view in front of the bike, and a angle ϕ of 10 degrees, the torso angle θ is found to be 40 degrees. Of course, once the fairing is put on, the vision angle will be somewhat decreased, but that is a function of the fairing construction, not of the pilot position.

It is important to analyze what does changing the main dimensions of the bike involve. The following table presents a qualitative description of what these changes involve.

Quantity	Direction of change	Effects
Height of Bottom bracket	⇑	• Better ground clearance in turns • Less vision angle, needs to raise the eye-level as well
	⇓	• Better aerodynamics due to less frontal area • Less ground clearance, can bottom out during a sharp turn • Can have lower eye-level
Height of hip	⇑	• Higher eye-level, better visibility • More horizontal leg at extension • Can achieve same eye-level with more horizontal torso
	⇓	• Less visibility due to lower eye-level • The leg is moving upward when on power stroke
Body angle	⇑	• Better vision due to higher eye-level • More comfortable • More power
	⇓	• Requires more hip height to achieve same eye-level • More comfortable • Better aerodynamics

The table was used to understand how to change the design of one of the prototypes we had, to obtain a better design for the race bike. Also the table will be used to understand which direction the design should take next, for the subsequent race bikes.

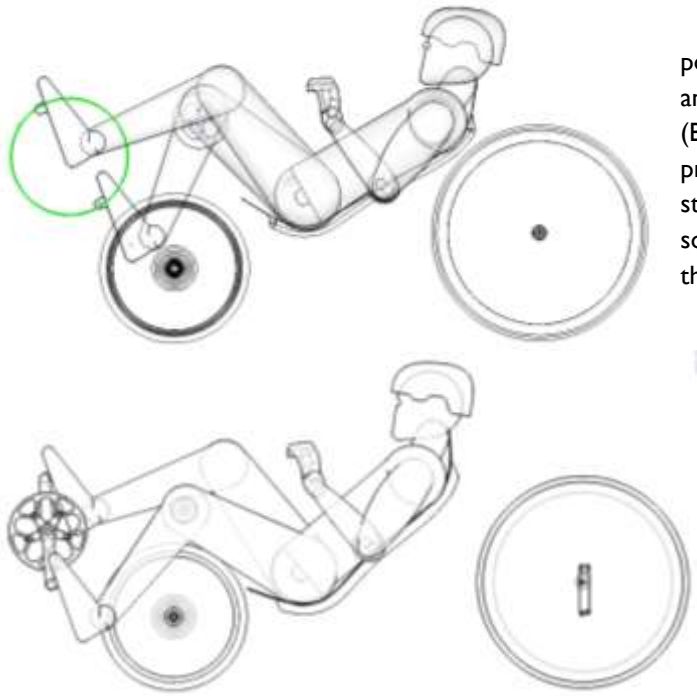

Figure 1 Comparison for Pilot positions

The pictures on the left indicate the rider position for the prototype we have built (on TOP) and the final rider position chosen for the race bike (BOTTOM). Due to the low eye-level of the prototype, the body angle was increased. The power stride of the leg was felt to push too much vertically, so the bottom bracket was lowered with respect to the hip height.

Requiring a lean angle of 40 degrees allowed the bottom bracket and seat height to be both lowered compared with the prototype.

The following pictures show the final dimensions for the race bike rider position.

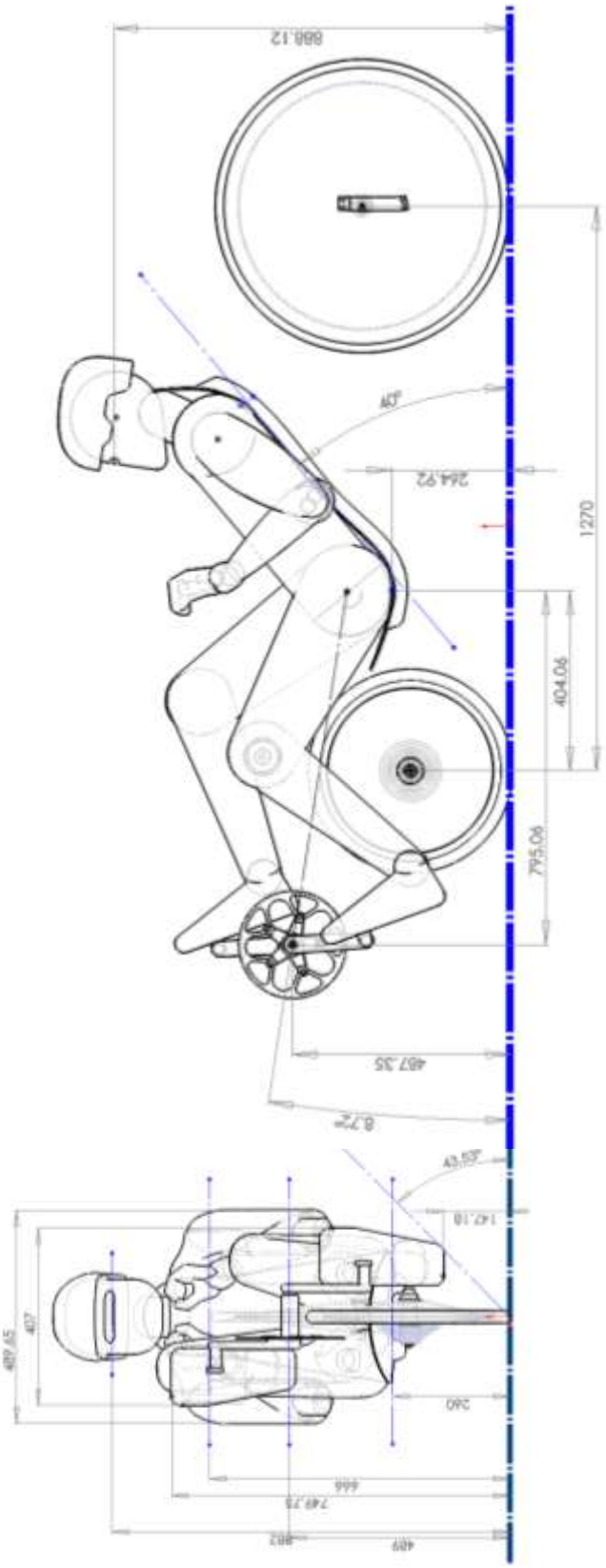
45°
264.92
1270
404.06
795.09
487.35
8.72°
43.53°
142.10
407
489.45
240
666
749.73
409

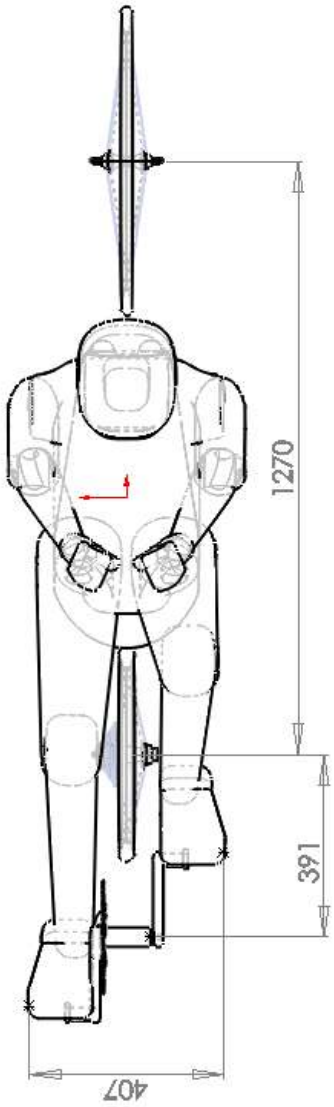
1270
391
407

3.4 Design for Structural Performance, Composite Primary Structure & Fairing

The design choice was made to incorporate much of the primary structure of the HPV into the aerodynamic fairing itself. This class of structure is called a "monocoque", or shell-structure, and the thin outer shell is responsible for carrying the loads applied. This choice was made for the following (somewhat sequential) reasons:

1. Given the previous experience of the HPVDT, it was a natural choice to use composite (especially graphite) materials where possible, due to their higher specific strength and stiffness when compared to isotropic materials (such as aluminum or steel).
2. Composite materials, by virtue of their pre-cured formability, can be made to conform to almost any geometry of structure. They can be as (or more) easily adapted to create a large hollow "Bathtub"-like cavity as they can a tubular frame structure.
3. Because an aerodynamic fairing with complex curvature was required, from an ease-of-manufacture point-of-view a molded composite shell seemed the most mass-effective option (e.g. versus paper-mache, lightweight-foam, bent sheet-metal, etc.).
4. Any aerodynamic shell, regardless of the internal primary structure, could essentially be designed to be self-supporting if made of a uniform thin laminate. However, with minimal weight additions, the incorporation of a structural core (either over the entire area or in local reinforcements) can add considerable stiffness to the shell, and in fact yields exponential gains for the specific-stiffness and strength of the structure. In addition, with the required depth of the bottom fairing-half for example, the geometry itself was best lent to incorporation into a beam-like structure (where the height of the beam is a critical factor).

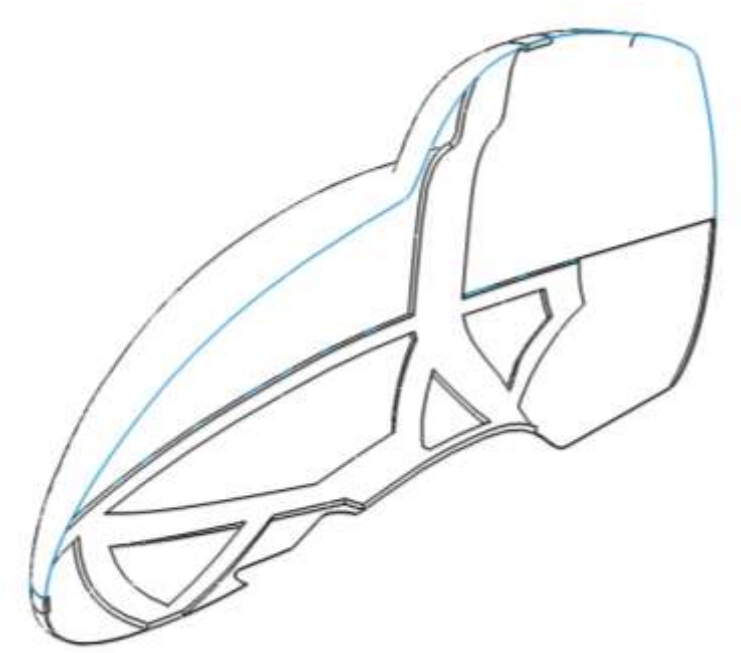

Figure 2 Cross Section of the bike structure

From a composites point-of-view, this is how the monocoque sandwich structure fairing was arrived at. Local sandwich reinforcement was selected because by strategically placing structural foam-core and additional composite reinforcement the load-paths could be tailored to take the most advantage of the geometry of the shell, and therefore considerable weight could be additionally saved. Because the fairing would be split into two parts for driver access, the structure could be incorporated into one or the other or both together (with some form of joining mechanism). Using the bottom-fairing alone seemed the best option, as it was smaller in overall area (e.g. large unsupported surfaces which could deflect under load), naturally underneath (and therefore supporting of) the occupant, and could best incorporate hardpoints for wheels, seat, etc. The top fairing would be designed to be self-supporting only.

The bathtub structural design began from an analogy to a beam-bending problem. In essence, in normal operation the HPV structure is a simply-supported beam, responsible for conveying the mass of the occupant to the wheels at either end. In beam design, the most mass-effective design is that which places the most mass furthest from the centroid of the structure, as this provides the greatest second-moment-of-area, and hence greatest bending stiffness per unit of material. Therefore the additional composite plies and structural

reinforcement were placed at the extreme bottom surface and extreme top edge of the bathtub. The bottom "flange" of the beam, similar to a boat keel, passed from the front drivetrain mount point, around the wheel-opening, to the rear drivetrain mount point, under the pilot, then finally up to the back wheel. The top "flange" is created by a gunwhale-like structure, which runs along the top edge of the bathtub along either side and is joined to the keel at either end. There are several reinforcing stringers between the keel and gunwhale along the beam's length in order to prevent excessive deflection of the non-sandwich surfaces in the case of the vehicle coming down on its side.

The roll-cage was designed to take advantage of the reinforced structure around the occupant, as that is approaching the area where the beam structure consolidates for the wheel support. The roll-cage is largely a hoop-structure, incorporating two columns, one vertical and one horizontal. The hoop's primary role is to deflect/support any loads that may be imposed on the occupant, and transfer these loads to the two columns. Again, for mechanical simplicity this entire structure was integrated with the bathtub alone and not the top fairing (the top fairing fits snugly overtop of the roll cage).

3.5 Design for Manufacture, Moldmaking

Historically, composite molded parts like boat-hulls have been made over hand-made molds, especially in low-budget applications. These molds have been made by making "lofts" or sections of the desired shape, fixing then at a regular interval, and filling/sanding between them to obtain a smooth surface. However, because of the large amount of hand-finishing (e.g. filling and sanding) involved, it is often difficult to obtain dimensional accuracy. This is a major shortcoming of home-built composite techniques.

Given the modern CAD tools available, generating a computer model of the vehicle was preferred for design and analysis (e.g. structural analysis of the monocoque frame and aerodynamic analysis of the fairing). In fact, it was also understood that with this model in hand, it would be possible to pair it with CNC tooling techniques in order to machine a mold to exactly the desired shape. This method is not entirely novel, but for those who can afford it is becoming more popular due to the reduced number of man-hours required and increased fidelity.

With this objective in mind, it was necessary to secure the material and facilities required for CNC machining of the mold. For this application, in which only a few iterations of the parts would be manufactured, a mold made out of medium-density foam is generally sufficient. A suitable quantity of an appropriate material, Renshape 460 Tooling Board, was obtained as a donation from the manufacturer. In addition, the team was able to secure donated CNC machining time from a local mold manufacturer, for the actual production of the HPV molds.

The molds are currently in production, and after fabrication, the largest surface deviations should be on the order of 1/32". The steps required thereafter will be light sanding (to bring the surface to its final smooth finish) and sealing (to prevent the adhesion of any of the epoxy matrix to the mold). This will again represent a much smaller time-investment than historical methods.

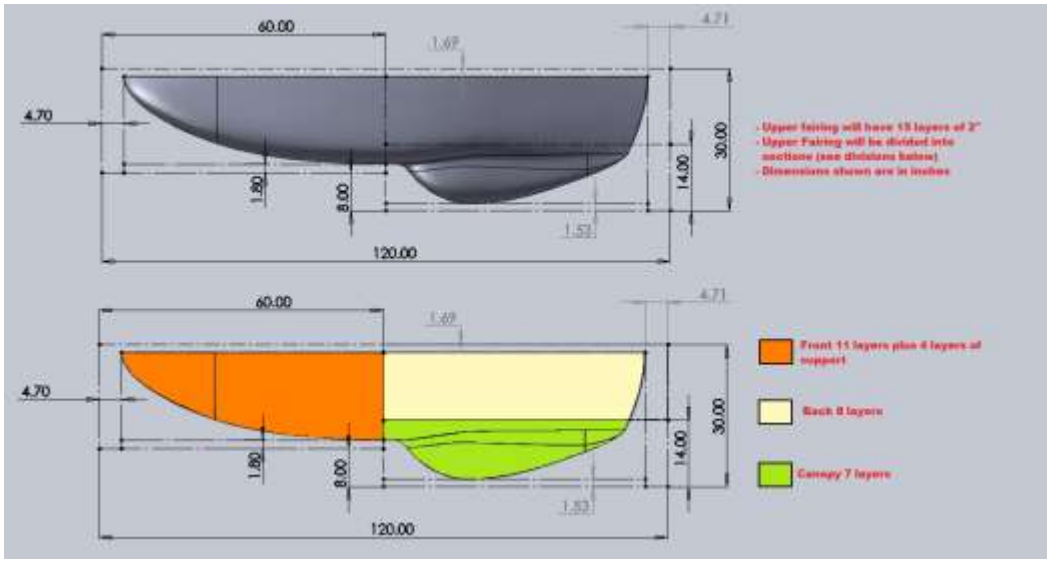

Figure 3 Upper Fairing Mold Dimensions

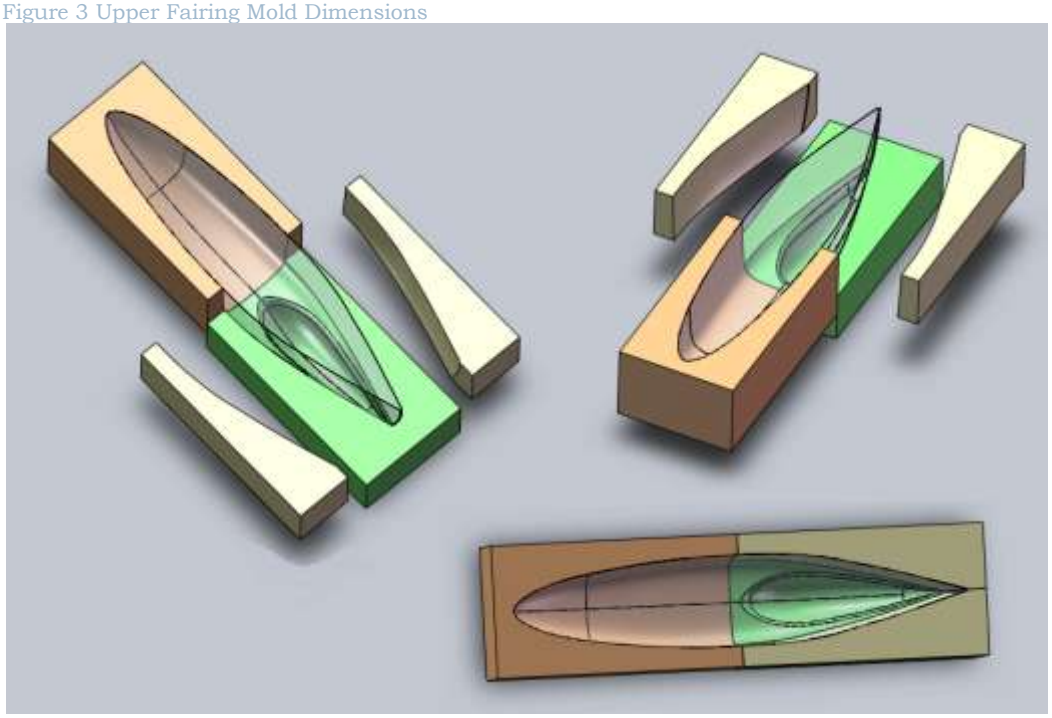

Figure 4 Top Fairing Mold Assembly

3.6 Design for Manufacture, Materials and Fabrication

The material technology chosen for the bathtub structure and fairing was, as mentioned, epoxy-matrix composite, with woven and unidirectional graphite being the particular material choice. Graphite, when available, provides significant structural efficiency far in excess of other composites. That being said, Kevlar does provide advantages for abrasion resistance and specific toughness, and may be incorporated locally into the structure after abrasion testing has been conducted.

Composite materials provide the unique advantage that it is possible to tailor their strengths advantageously through thoughtful orientation of the fibers to best sustain the local load. In some cases (e.g. the hoop structure), it is ideal to use predominantly unidirectional material, where the load directions are very clearly defined. However, in most cases biaxial-woven graphite was used because it was more available and in general the load path through the bathtub structure and fairing were less well defined.

There are a dizzying number of options available for composites processing, including (in order of structural performance) wet-layup, vacuum-bagging, resin-infusion, and pre-impregnated ("pre-preg"). Wet-layup yields inconsistent and poor material properties, but is the easiest, whereas pre-preg fabrication yields the most consistent and highest performance, yet is the most expensive. Resin-infusion Molding (RIM) processing was chosen in the end because:

1. The fibre-fraction achievable with RIM is very close to that of pre-preg, at 60-65% (close to the theoretical maximum).
2. RIM allows more time to position different materials and plies as in the structure to be fabricated here (e.g. complex layouts of foam reinforcing-core, unidirectional plies, etc).
3. RIM is similar in cost to wet-layup and vacuum-bagging, but higher-performance than either.
4. RIM can achieve a lower percentage composition of air pockets ("voids") than either wet-lay or vacuum-bagging, which provides for the smoothest exterior surface finish and lowest viscous drag.

The resin-infusion fabrication process begins with the positioning of dry composite materials inside the mold. In this situation, a sandwich structure, the outer plies will positioned first (directly against the mold), then the structural foam-core reinforcement (held in place with a light adhesive spray), then the interior plies over the foam-core. Because there is no epoxy involved at this stage, there is no time limitation involved in positioning the materials. After everything has been satisfactorily positioned, infusion media (a thick plastic mesh that allows flow of the resin over the part) and infusion lines (positioned along the spine of the mold for resin ingress and around the perimeter for drawing vacuum) are positioned. Finally the entire assembly is sealed against the mold using vacuum bagging film taped along the mold edges. When vacuum is applied, resin is infused along the ingress lines in the spine of the mold, and pulled uniformly outwards towards the vacuum lines. Eventually, The entire laminate has been infused with resin and the infusion lines can be clamped shut, while the part is held under vacuum until the resin is hardened. This ensures that the part will consolidate and cure in as dense and void-free a state as possible.

3.7 Transmission Design

The transmission was designed to be as efficient and modular as possible. A intermediate drive has been built, and allows for simple and fast gear changes. A Dura-Ace 9 speed derailleur and cassette will be used to select the correct gear.

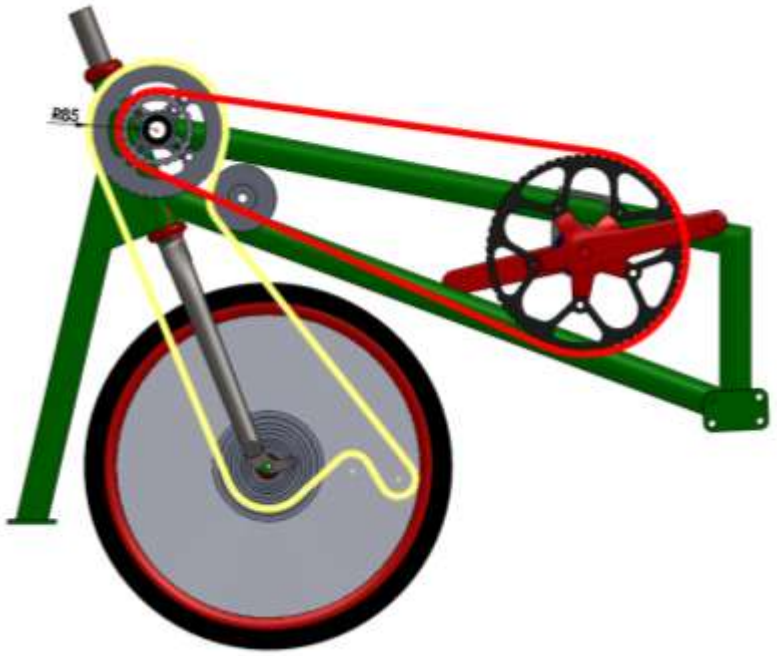

4 Analysis

4.1 Roll-cage Structure

The most crucial component for structural analysis was the roll-cage and associated driver-protection structure. The hoop itself was modeled in Solidworks Simulation as a sandwich-structure, with plastic-foam core and carbon-fiber facings, and analyzed independently of the rest of the primary structure. This hoop is aided with the addition of cross-member, also modeled as carbon fiber, to more effectively transmit the required loads. For maximum structural efficiency, the hoop reinforcement will incorporate unidirectional carbon in the circumferential direction, as this material will have the highest specific strength and stiffness for a known load path. For simplicity, in Simulation this material was modeled as having isotropic properties. These properties were determined from a previous HPVDT project, and are as follows:

Elastic Modulus, E	1.843E11 Pa
Compressive Strength	1.810E9 Pa
Tensile Strength	1.86E9 Pa
Density	1.86E3 Kg/m^3

These properties are from a standard modulus fiber very similar to that to be used on the primary structure, as well as an epoxy matrix from the same manufacturer with similar properties to the desired infusion epoxy. However, these properties will be updated and the testing re-iterated once the exact laminate properties have been determined from a test part.

The factor of safety for the 600lb vertical load was 340, and the factor of safety for the 300lb horizontal load was 27. A more detailed analysis will be performed, and a test will need to be performed to make sure the roll cage is strong enough.

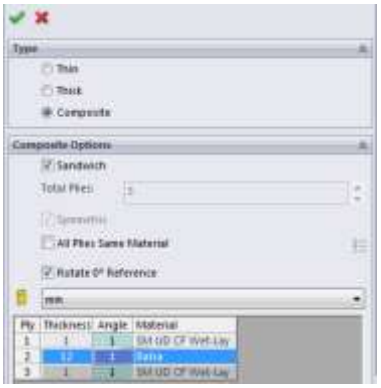

Figure 5 Sandwich structure definition in SW2010

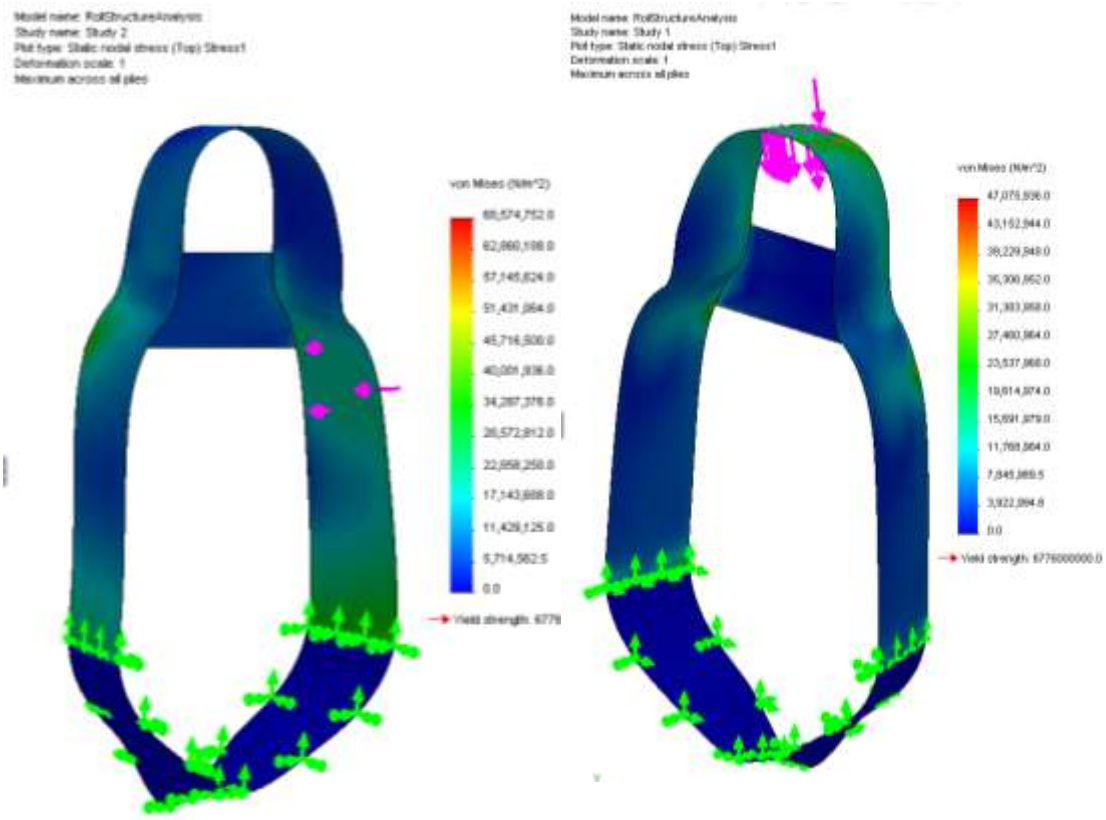

4.2 Analysis, Bathtub Structure and Fairing

The bathtub structure and fairing are comprised of an orthotropic carbon fibre weave laid up over a complex structural geometry, which is considerably different from the well-defined and easy-to-model hoop structure examined previously. This must be analyzed with a full membrane analysis FEM with the ability to handle composite materials. One approach which shows promise is the use of Hypersizer to mesh a model with the correct geometric and material properties (e.g. multi-ply laminate with local structural-foam reinforcement), and carry out the FEA itself with FEMAP, a commercial finite-element code. However, the pairing of these two analysis steps has not been carried out successfully yet, but work continues on this and success is expected before the fairing is ready to be infused.

The loads to be modeled on the bathtub structure include the gravity load imposed by the occupant as well as the reaction loads from the wheels and drivetrain, which have previously been modeled using Solidworks Simulation. These were determined by careful calculation and analysis and should prove adequate for this situation also.

The design decision was made previously that the top fairing would not comprise a significant portion of the primary structure, and would merely provide an aerodynamic shell. In this vein, it is therefore required only to resist the aerodynamic drag and side loads placed upon it (for example in the 15 m/s forward velocity and 15 m/s forward & 5 m/s sideways cases). If the exact aerodynamic load profiles cannot be applied, a representative load will be applied instead.

Analysis of Frontal Structure

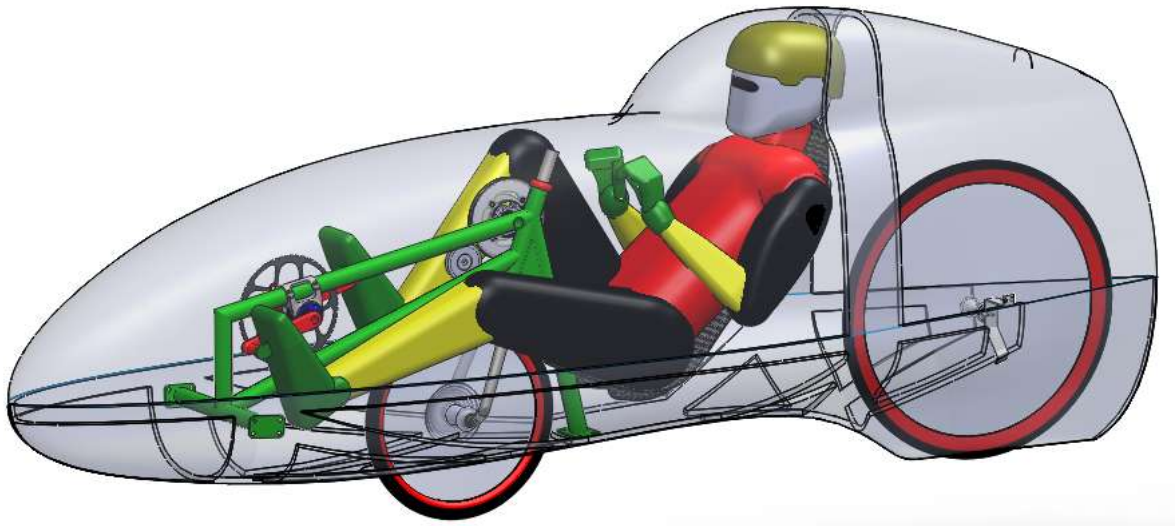

The frontal structure is a welded aluminum structure (GREEN) which is bolted to the bathtub structure, and supports the pedals and the front fork, as well as the transmission pulleys and intermediate drive.

The front structure is made of 1/16 in thick 1.5 in diameter 6061 T6 aluminum tubes. The head tube is machined such that a normal 1-1/8 in head tube can be press fit in. Two studies were performed, The first one has forces of 1000N backward and 1000N up applied at the point where the wheel mounting points of the fork,

simulating hard braking, as well as a force of 2000N pressed on the pedals. The minimum factor of safety was 3 for the welded aluminum structure.

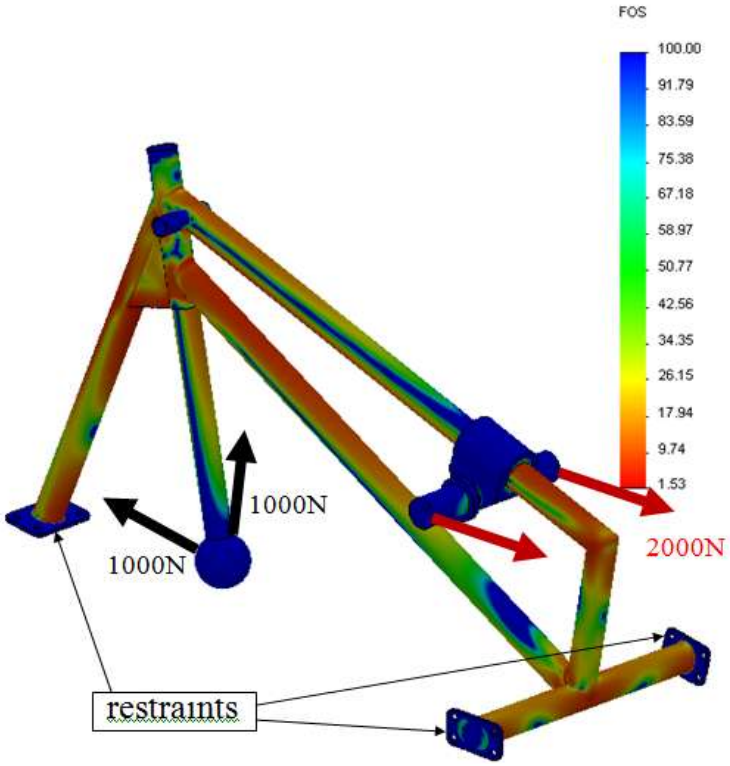

The second test has a 800N force applied at the pedals, corresponding to a 600N chain tension. A minimum factor of safety of 3.3 was obtained for the aluminum structure.

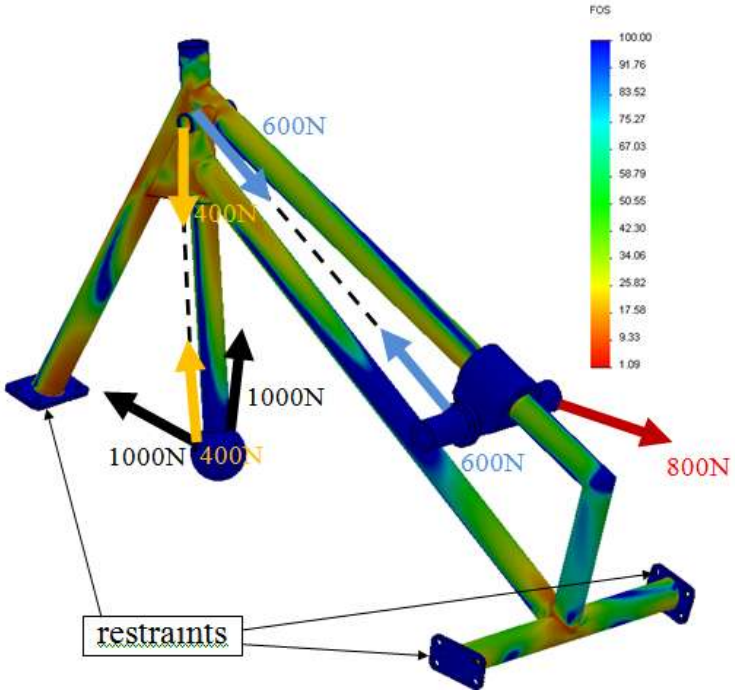

5 Testing,

5.1 Primary Structure Proof-loading

The mold for the primary structure is currently being manufactured, and the primary structure layup will be conducted shortly thereafter. The test schedule and proof-loading regime to be carried out is as follows:

1. 600lb Roll-Cage proof-load: Apply load as specified in competition rules, and confirm that the structure survives and does not deflect such that the driver is encroached-upon.
2. Full-Power Proof-loading Interference Testing: The vehicle will be secured on a stationary bike mount, and full-power applied by a driver. The structure and fairing will be observed to ensure that there is no interference between the driver's body and the structure, as this could cause discomfort, a loss in performance, etc.
3. Static Deflection of Primary Structure: The deflction of the bathtub structure will be observed while the driver is seated inside the vehicle. This will be used as a validation measure on the to-be-performed fairing analysis.

5.2 Testing, Composite Manufacture

The team has so far produced a test layup for the resin infusion technique to be used in production of the HPV primary structure. The infusion involved a 3-layer woven graphite fabric and an off-the-shelf infusion epoxy, PTM&W PR2712. The laminate was infused over a length of 24", which is the longest possible diffusion distance expected in the final top-fairing layup.

The results of this layup were extremely positive. The epoxy was able to infuse over this distance in only 8 minutes, which, given the epoxy takes 45 minutes to "gel" (after which it will not flow), will be sufficient. Also, the infused laminate was compared with the dry-fabric weight prior to infusion to determine a fibre content of roughly 65%, which agrees with the best-case prediction and proves promising in terms of performance. The part also had a surface finish on the tool-side (e.g. that adjacent to the mold) which perfectly mimicked the finish of the tool-itself, i.e. a mirror-finished buffed surface (ideal for the vehicle's aerodynamics). This experience and that of the team's advisors (with considerable experience in composites fabrication) provide confidence that the final structural components can be fabricated to specification.

A local composites manufacturer has agreed to donate the use of their material testing facilities for the team's determination of laminate properties for this as-built specimen. As mentioned, the current properties being used were those determined experimentally in a prior design project, but as these new properties are obtained they will be substituted-in and the design iterated.

6 Aerodynamic Design

The goal of the aerodynamic design is to reduce drag by eliminating sources of flow separation, minimizing wetted area, reducing wheel drag with appropriate fairings, reducing junction drag with appropriate fillets, reducing gap drag by sealing wheel wells and seams, and extending runs of laminar flow over the nose region. The shell is constrained by the shape of the rider, the need for ventilation, and limits on the convexity for the purpose of mold construction and release.

Preliminary estimates indicated that despite the added weight, a fully enclosed aerodynamic fairing would give the best score in both the drag race and endurance race. Ease of manufacturing was considered, but given the experience and dedication of the team it was decided to design a fairing with minimal aerodynamic compromise. Tamai's "The Leading Edge" (Ref. 1) was used as the primary resource while designing the fairing and computing the preliminary drag estimate. The design of the various parts of the fairing is described below along with the estimated drag values given in Table 1.

The shape of the main shell was determined primarily by the position of the rider, pedals and wheels, which were chosen based on an existing low-rider recumbent bicycle known to have excellent handling qualities. The shell was fit as closely as possible to the rider, using an accurate CAD model of the rider anatomy as shown in Figure 1. To prevent flow separation the angle of the shell in the pressure recovery region, as seen from the top view (Figure 2), never exceeds 17°, which is the rule of thumb for vehicles operating in this range of Reynolds numbers. The shell was made as narrow as possible and changes in curvature made as subtle as possible to reduce supervelocities on the surface. The seam was placed on the stagnation point and seam line placed such that the curvature of each half of the mold would be fully convex. The width was increased gradually to its maximum value around the pilot's shoulders in order to set up a positive pressure gradient promote extended laminar flow. In reality the flow may only remain laminar over the first 20% of the fairing length, but this still results in a 6% reduction in total drag. Truncating the tail, instead of having it come to a sharp point can reduce drag by reducing the total wetted area. Prof. Mark Dela of MIT suggests a rule of thumb where the flat base area of the tail is ¼ the drag area of the vehicle, which results in a width of approximately 1cm, and a reduction in overall length of 4cm.

The drag of the main shell was estimated using the boundary layer equations and torpedo-flat-tail model presented in Tamai's book, combined with the surface area measured from the SolidWorks model. It was found to have a drag area of 0.0119 m^2 at the reference speed of 15 m/s (54 km/hr).

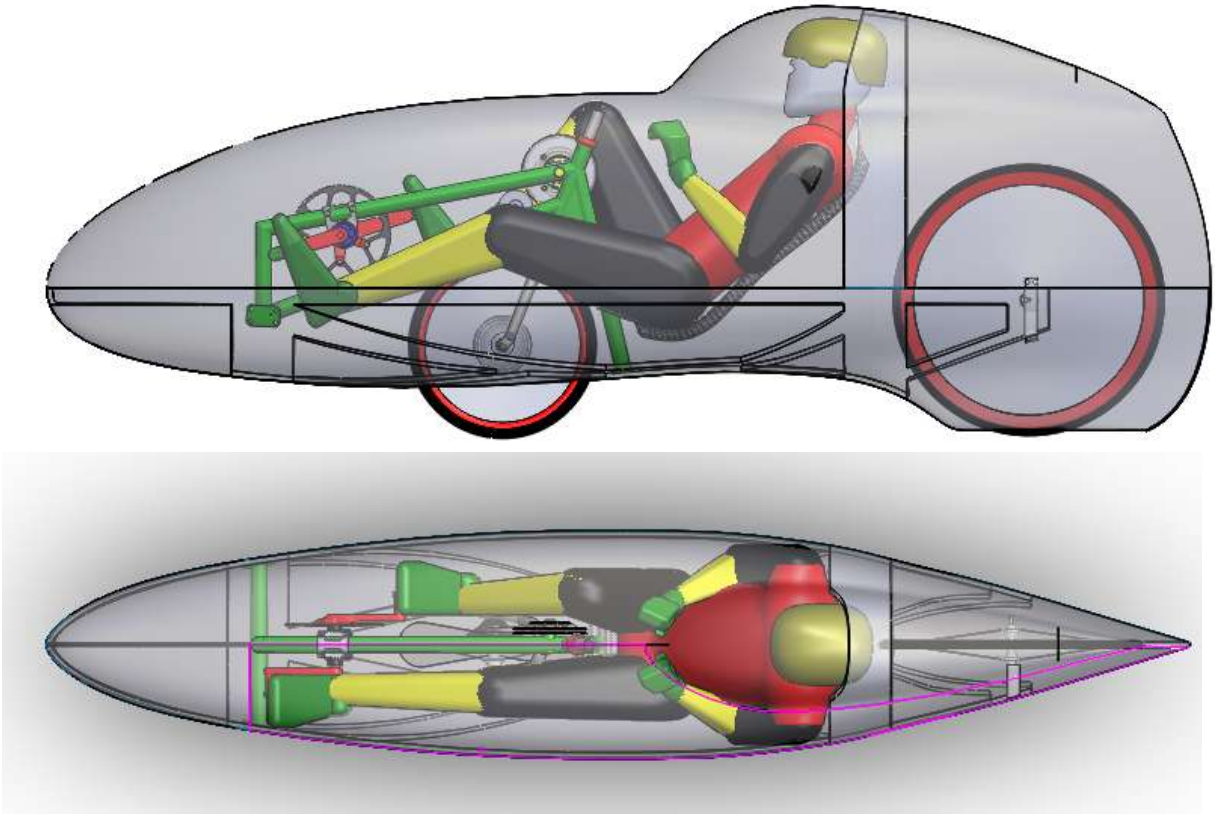

The canopy was designed to give adequate visibility and mobility of the head while minimizing it's protrusion into the flow and preventing flow separation. Horseshoe separation on the front on the canopy is prevented by adding a significant fillet. The rear of the canopy is tapered slowly, never exceeding 17° in top view or side view to prevent separation on the leeward side. Junction drag is minimized by filleting the sides. Using this design strategy, Reference 1 was used to estimate the drag area of the canopy at 0.0024 m^2 at 15 m/s.

The rear wheel fairing is designed as a full fairing with a large fillet on the leading edge to prevent horseshoe flow separation. The hole in the bottom of the shell will be cut as close as possible to the wheel to minimize air exchange between the exterior and interior of the shell, thereby minimizing drag loses. Since the front wheel must steer it was decided that the best compromise between ease of construction and drag reduction was to have two have fairings in front and behind the wheel (not shown in the figure). These will be made of foam and added after the shell is completed. The hour-glass cutout in the shell that allows the wheel to steer will be sealed with a thin plastic, again to minimize air exchange and drag. Using Reference 1, the drag area of the rear and front wheels at 15 m/s are 0.006 m^2 and 0.012 m^2 respectively. Note that the drag of the front wheel is equal in magnitude to that of the main body itself.

Ventilation will be provided by the small amounts of air that leak through the wheel openings. If this does not prove adequate during testing, a small slit will be added to the front of the canopy, in a high pressure region of the flow. The ventilation flow will exit though a 1cm x 5cm slit in the top of the trailing edge. Entering in a high

pressure region, focusing the flow on the neck and head, and exiting at a low pressure region will provide the most cooling with a negligible drag penalty.

A summary of the drag breakdown is given in Table 1. The total drag area for the vehicle is estimated to be 0.0323 m^2, which corresponds to a drag coefficient of C_d=0.079 based on a frontal area of 0.408 m^2. At the reference speed of 15 m/s this corresponds to a drag of 5.7 N and a required aerodynamic power of 85 Watts. Due to Reynolds number effects on skin friction drag, the drag coefficient is not constant with speed. The effect is the most pronounced on the main body and has been incorporated into the aerodynamic model as shown in Figure 3.

Fairing Part	*Drag Area at 15 m/s (m^2)*
Main Body	0.0119
Canopy	0.0024
Rear Wheel	0.006
Front Wheel	0.012
TOTAL	**0.0323**

Table 1: Drag areas of the various fairing parts at 15 m/s, computed using the "built-up" method described in Reference 1, assuming 20% laminar flow and using the exact fairing geometry computed from the SolidWorks model.

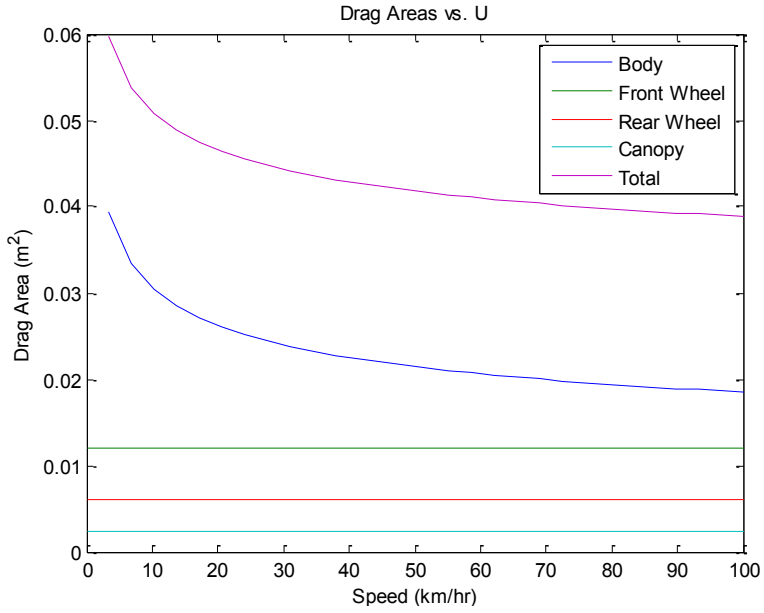

Figure 3: Speed dependence of drag areas as modeled using the built-up method. The additional drag of the canopy and wheels is assumed to be Reynolds number independent.

As a double check on the drag results, the drag of the SolidWorks model was computed in Cosmos Flow Works for the zero wind condition, and a 5 m/s cross-wind condition, both at a ground speed of 15 m/s. The results are shown in the Figures below.

The model was run with fully turbulent flow, and without the front wheel fairing, which partially accounts for the high drag force of 11.2 N, which nearly twice that calculated using the method described previously. The final drag results will likely lie between these two extremes, but determination of the exact value will have to wait for field testing of the actually vehicle. The CFD results, however, do show that the flow is fully attached, reaffirming the design decisions regarding the amount of taper on various sections.

Two tests were conducted, the first is 15m/s speed with no cross wind, and the second is 15m/s speed with 5m/s cross wind. In both tests the ground was modeled as a moving wall, moving back at 15m/s. The next page represents the results of the test with no cross wind.

The main reason for performing the CosmosFlow analysis is to obtain a qualitative understanding of the flow around the bike, and figure out if and where separation might occur. The numbers obtained for the drag forces are important, but need to be checked versus the analytical model, and against the results of the real bike.

6.1 Aerodynamic testing using Cosmos Flow

6.1.1 15m/s velocity

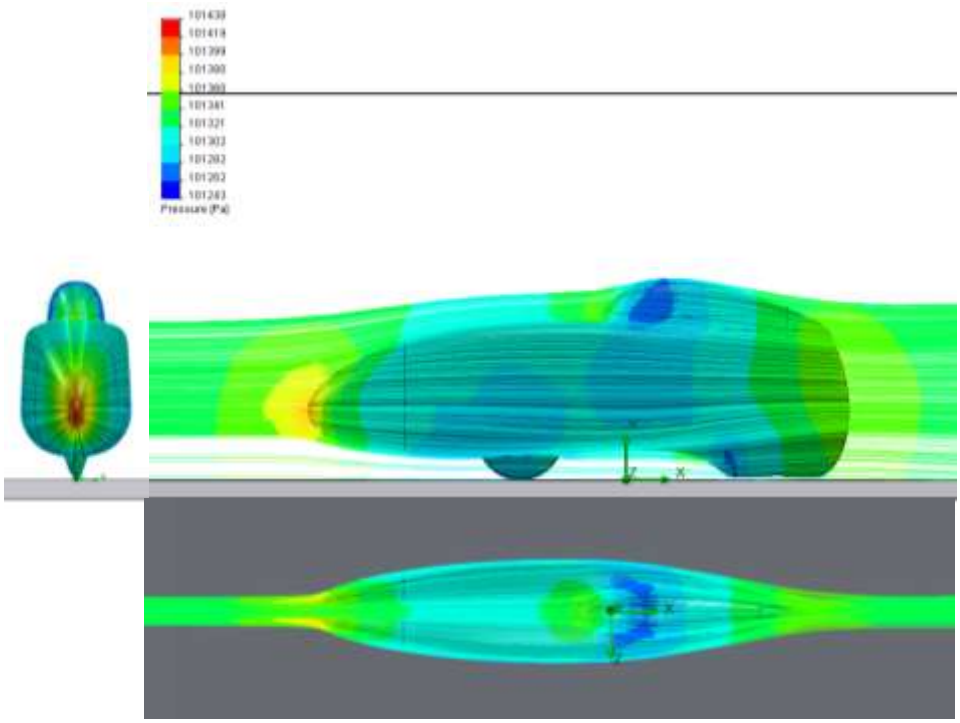

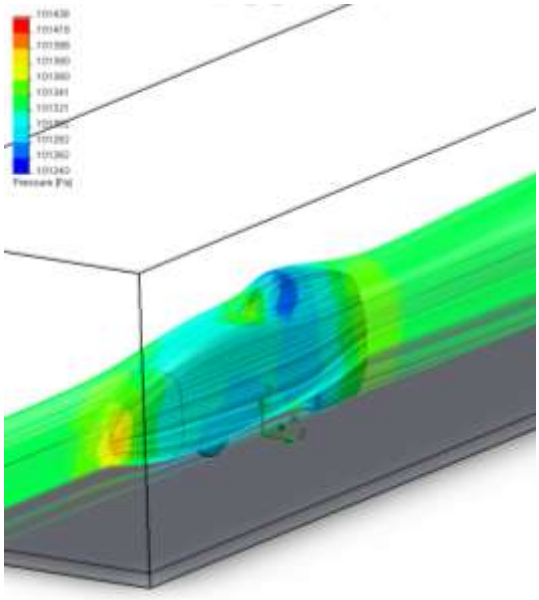

Goal Name	Unit	Value
GG X - Component of Force 1	[N]	11.21726362
GG Y - Component of Force 1	[N]	-3.398096972
GG Z - Component of Force 1	[N]	0.076017733

Figure 6 15m/s speed simulation

6.1.2 15m/s with 5m/s cross wind

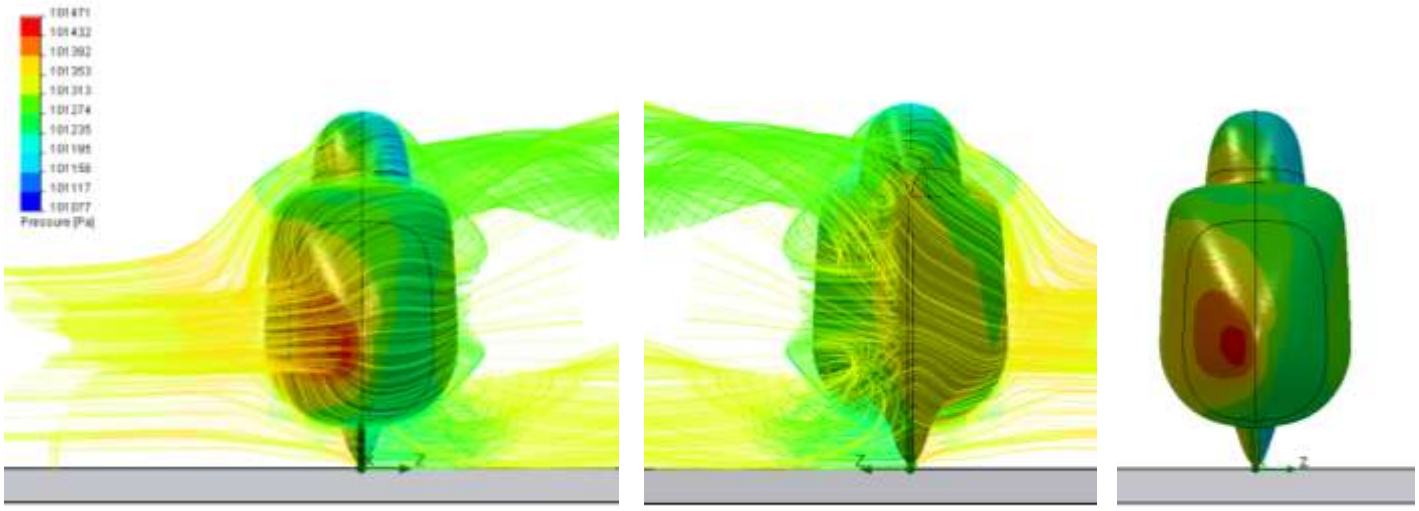

It is interesting to see how the maximum pressure area changes from the frontal area of the bike to the right side, given a cross wind from the right. Also the flow presents interesting vortices being formed behind the bike, one on the top, behind the canopy, and one in the bottom, behind the rear wheel.

The simulation also shows small areas of flow separation behind the front and rear wheels, but no major separation on the body of the bike.

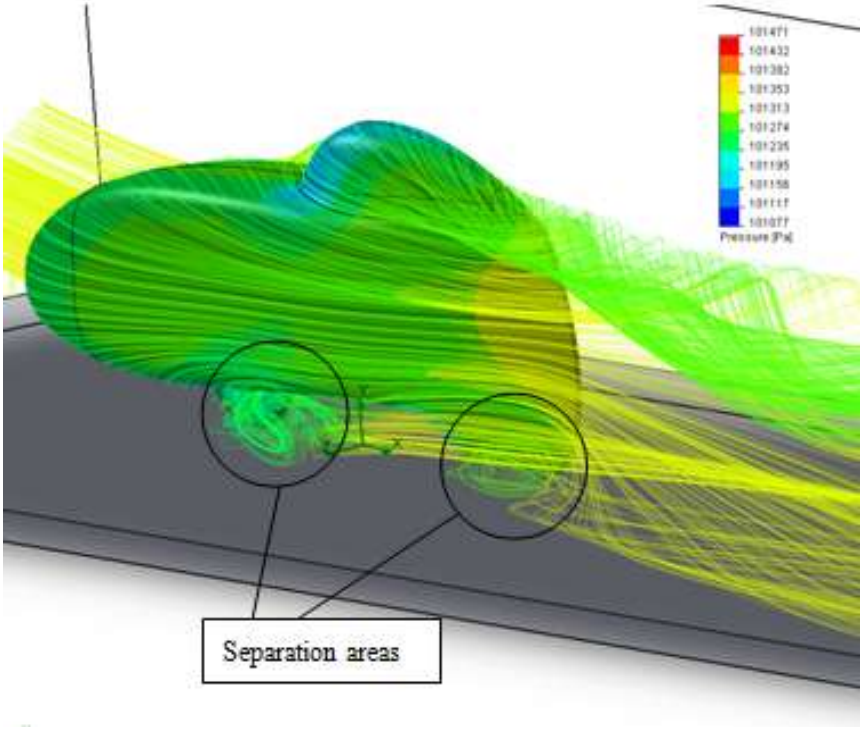

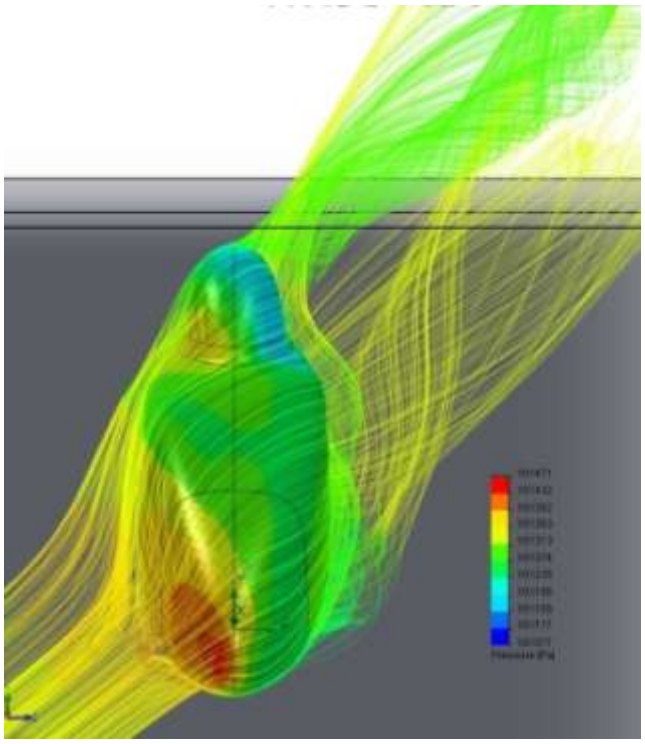

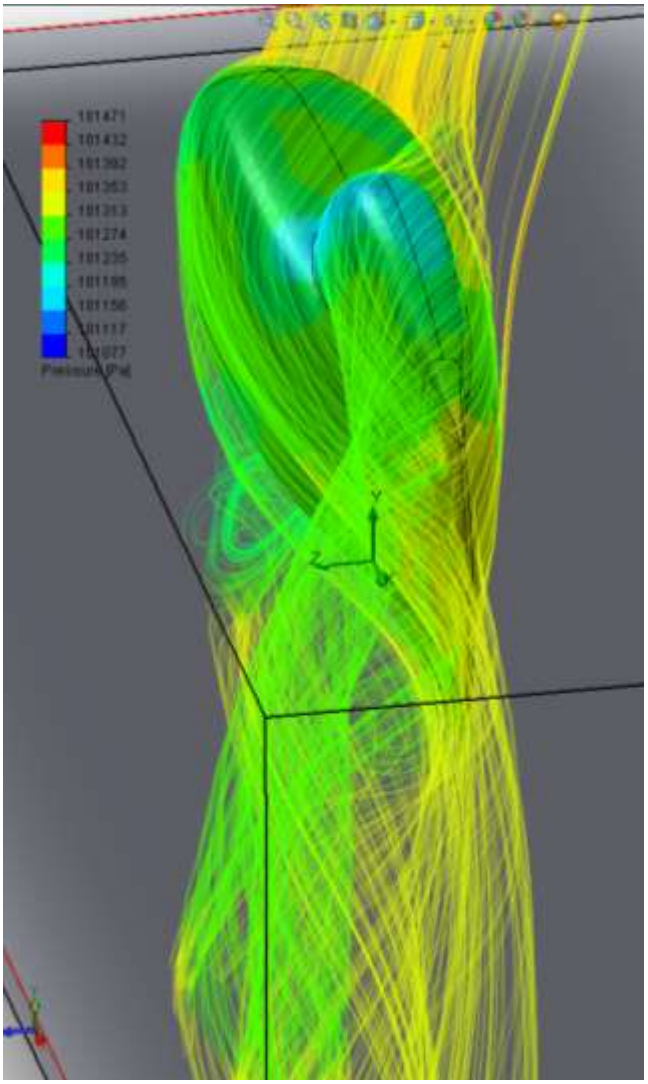

Goal Name	Unit	Value
GG X - Component of Force 1	[N]	10.28476227
GG Y - Component of Force 1	[N]	-38.24249927
GG Z - Component of Force 1	[N]	111.7742231

It can be seen that the force along the X direction (the direction of motion) is 10.2 N for the cross wind case, and 11.2 N for the case with no cross wind, meaning that the cross wind causes 10% less drag than the no-cross wind case.

The force in the Z direction is 111N for the cross-wind case, which means there might be big maneuverability problems for such a big cross wind.

In conclusion, the fairing has been designed with very few aerodynamic compromises. Analytical models and empirical data from Reference 1 were used to quantitatively select the lowest drag solution for each of the sub-components of the fairing. Surface finish of the nose will be critical to maintaining laminar flow, but in practice, it will be of little consequence beyond the first 20% of the fairing's length. Though the analytical model does not correspond exactly with the CFD results, both models are within reason and provide a good starting point for the creation of a race simulation model.

References

Tamai, G. (1999), *The Leading Edge: Aerodynamic Design of Ultra-Streamlined Land Vehicles*, Bently Publishers, Cambridge, MA, USA

Hoerner, S. F. (1965), *Fluid-Dynamic Drag*, Hoerner Fluid Dynamics, Brick Town, N. J. USA

Mark Drela's quoted rules of thumb: http://www.recumbents.com/WISIL/barracuda/barracudafairingdesign.htm

7 Safety

As part of our analysis several safety factors were identified and addressed, these include; materials integrity, visibility restrictions, adequate communication, collision effects. To ensure a comprehensive design, at each step of the design the safety of the rider and spectators was considered with the highest degree feasible.

7.1 Materials Integrity

The materials integrity of the faring is important as it provides structural support (lower fairing only), aerodynamics and is the last line of defense between the rider and the pavement following a collision. Thus to ensure that the fairing is able to provide adequate protection for the rider performing several tests on the materials used in construction will be performed. The scenarios considered include; abrasion against the road surface and the mode of fracture during the breakage of the fairing material. Abrasion against the road surface was minimized through the use of Kevlar as the inner most layer of the fairing; this material was selected for its superior abrasion resistance. The degree of incorporating this material would be further determined during the abrasion testing where expected conditions will be simulated. If fracturing of the fairing material would occur it would be important the composite chosen not exhibit an explosive breaking property or have sharp edges as both of these scenarios may cause harm to the rider or individuals whom may come in contact with the damaged part. This hazard will be minimized through composite testing and the incorporation of specialized structural expoxy.

7.2 Visibility restriction

The awareness of the surroundings by our rider is paramount to avoid the possibility of dangerous situations such as collisions. Although optimally a low profile is desired in order to achieve maximum performance, design considerations have been taken into account in order to achieve a reasonable balance between safety and performance. From the design stage, when selecting the configuration of the vehicle, the importance of providing decent visibility was considered as a major decision element, ultimately leading to the choice of a recumbent type vehicle. Using a prototype vehicle and by artificially obstructing views a minimal angle of vision was determined and incorporated into our design equations. Furthermore the fairing windscreen opening was designed according to the regulations provided by the HPVC guidelines of allowing an unobstructed 90° view to either side of the rider.

7.3 Adequate communication

Providing the rider with live communication will not only allow information regarding the race to be relayed to them but will also allow us to give them a warning of hazards or dangerous conditions and having them discontinue if conditions are severe. This live communication will be accomplished by equipping our rider with a two way short range radios. This system can also act as a redundant safety system for situations where it is doubtful the rider would be able to view the danger from the canopy opening or in the case of a mechanical fault on the vehicle itself. Utilizing several spotters lowers the probability of a dangerous event.

7.4 Collision avoidance / minimization

As the designed vehicle will be operating in proximity to pit crew members, observers and other by standers, their safety is an important consideration in the design. In order to bring awareness and visibility to the design of the vehicle, our team has selected a paint scheme comprised of bright colors combined with dark colors, this both allows our vehicle to have a sharp contrast against all types of backgrounds.

The design of the vehicle itself has no sharp edges or elements in its fairing so that, in the unlikely event of a human collision injury can be minimized.

To provide protection to the rider a four point harness will be utilized to prevent the rider from injuring themselves on the inside of the vehicle. A four point harness was selected in order to provide adequate restraint under even severe collision conditions.

8 Power Curves and Race Simulation

An analytic model of the aerodynamic and rolling drag was developed with the purpose of simulating various race strategies. The goal was first to predict the performance of the vehicle, and second to adjust the race strategy for the best performance.

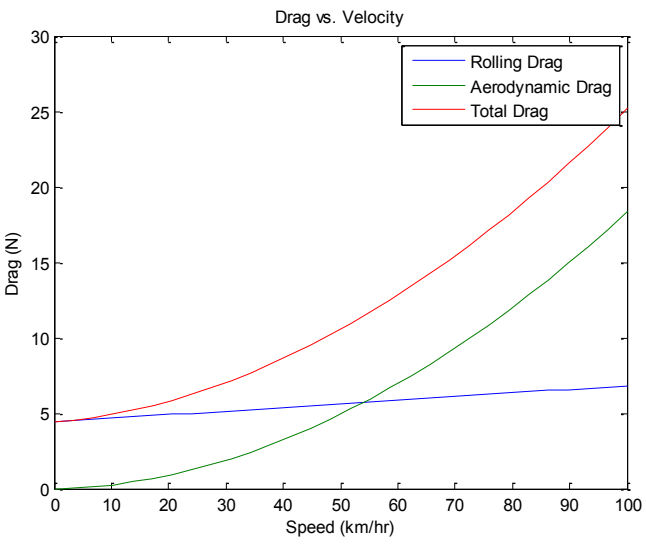

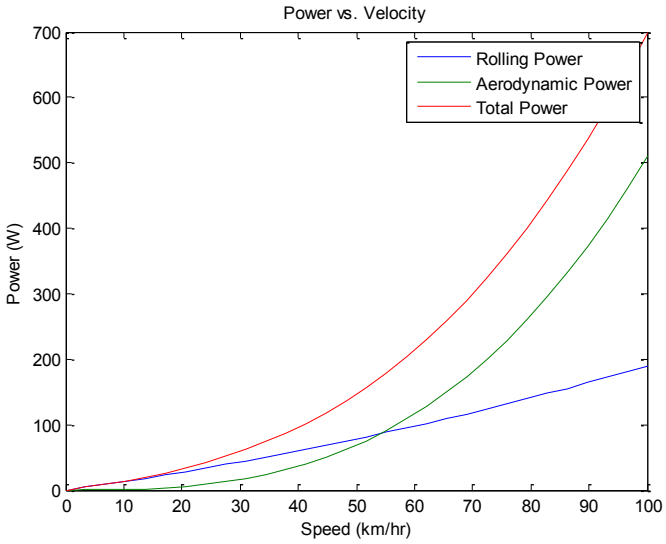

Figure 7 Speed dependence of aerodynamic and rolling drag Figure 8: Required power as a function of vehicle speed

The aerodynamic model is that described in the Fairing Aerodynamics section, and the rolling resistance model was taken from Reference 1, assuming a 100 psi bicycle racing tire. Figure 1 shows the contribution of rolling resistance and aerodynamic drag at various velocities.

A knowledge of the drag as a function of the velocity allows for a simple implementation of a time-marching algorithm to simulate either the drag race or the endurance race. Figure 8 shows the results for a drag race simulation where the pilot is able to maintain an output of 400 Watts for 60 seconds. The blue curve represents the "best case" half-fairing design, where only a tailbox is used to reduce aerodynamic drag. As a "best case" it was assumed that the vehicle would weigh half as much (purposely underestimated), and that the drag would only be 4 times as high (also underestimated). This simple simulation shows that after the first 20 seconds the full-fairing design, shown in green, has overtaken the half-fairing design despite the exaggerated "best case" assumptions. After 60 seconds the full-fairing is 70m ahead of the half-fairing, which was used as conclusive evidence that a full fairing should be used. The red curve shows a "power-managed" run, where the pilot uses the same total energy, but starts at 500W slowly decreasing the power output as the run progresses. This strategy shows a significant advantage over the constant power approach, indicating that it is worthwhile to use excess energy at the start to accelerate as quickly as possible, even if it drains energy and results in a much lower power output at the finish line. In the coming weeks, a more precise human-power model will be developed by testing the pilots on the ergometer with various power-time profiles to exactly how the total energy output is affected by an power spike at the start of the race. Applying a more accurate human model to the simulation will allow the team to determine the optimal power profile. If time and facilities permit, the technique will be further refined on the race bike.

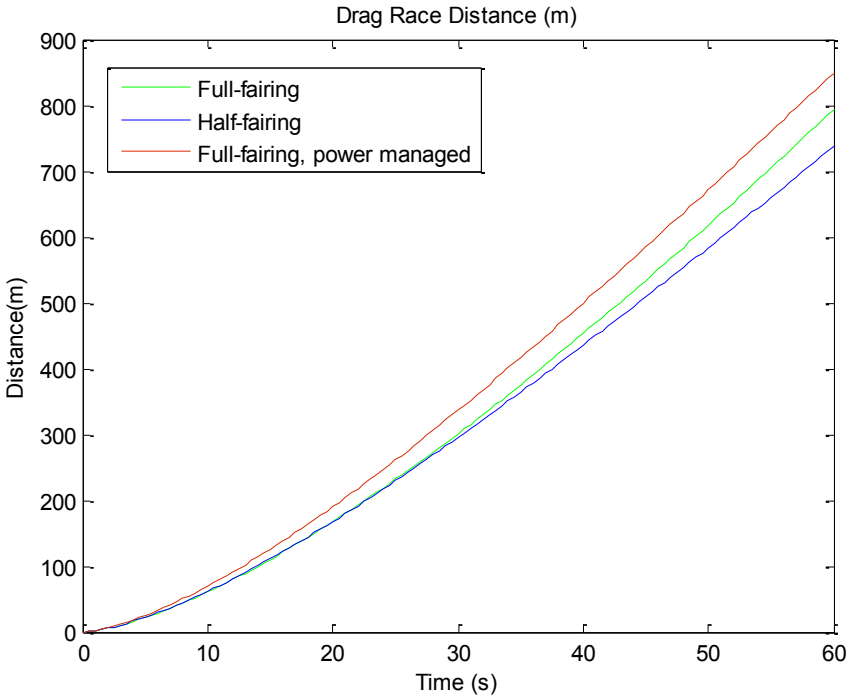

A simulation of the endurance event will include pit stop time and power models for the various pilots. Each pilot will be tested on an ergometer several times to determine their average power output for a 20 minute interval. The human-power model developed by the MIT Daedalus Human-Powered Flight Group (Figure 3) will be used to extrapolate each pilot's power output for longer and shorter distances. Using the constraint that no pilot may race for less than 5km or more than 20km, an optimal race strategy will be developed that results in the fastest overall time.

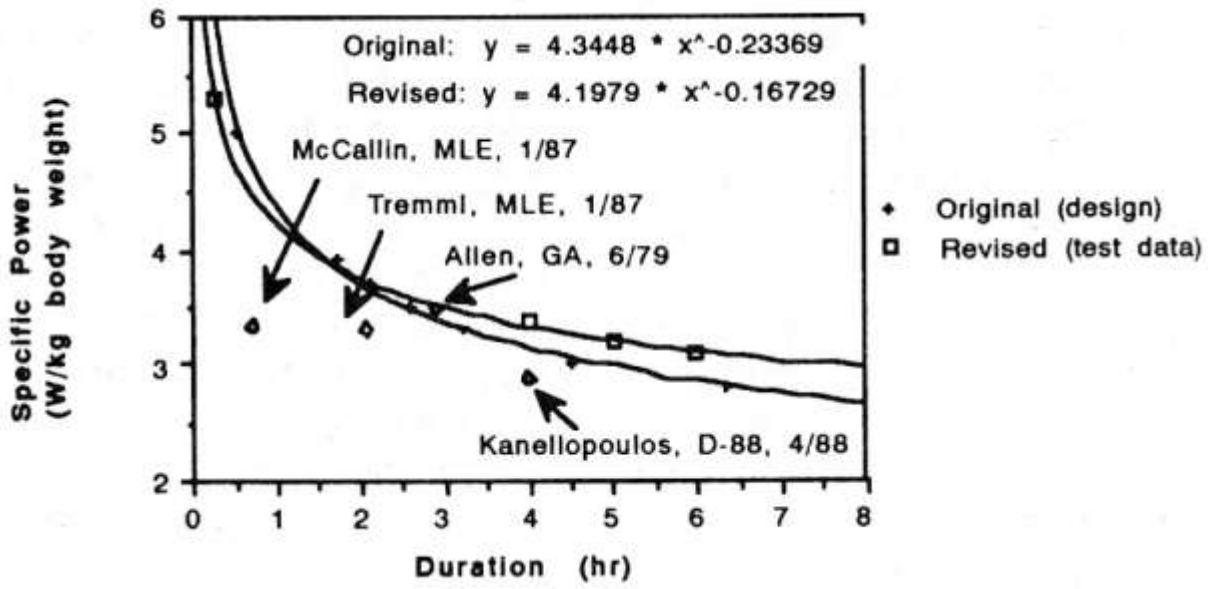

Figure 9: Human-power output vs. time from the MIT Daedalus team.

In conclusion, a semi-analytic model of the race vehicle is in the process of being combined with an empirical human-power model to predict race performance and determine the optimum race strategy for both the drag race and the endurance race.

References

Langford J., "The Daedalus Project: A Summary of Lessons Learned", AIAA Aircraft Design, Systems and Operations Conference, Seattle, WA, July 31 - August 2, 1989.